NeuroImage: Clinical 35 (2022) 103109

Contents lists available at ScienceDirect

NeuroImage: Clinical

journal homepage: www.elsevier.com/locate/ynicl

Myelin water imaging in relapsing multiple sclerosis treated with ocrelizumab and interferon beta-1a

Shannon Kolind [a,b,c,d,1,*], Shawna Abel [a,1], Carolyn Taylor [e], Roger Tam [b,f], Cornelia Laule [b,c,d,g], David K.B. Li [b], Hideki Garren [h], Laura Gaetano [i], Corrado Bernasconi [i], David Clayton [j], Irene Vavasour [b,1], Anthony Traboulsee [a,1]

[a] Department of Medicine (Neurology), University of British Columbia, 2775 Laurel Street, Vancouver V5Z 1M9, Canada
[b] Department of Radiology, University of British Columbia, 2775 Laurel Street, Vancouver V5Z 1M9, Canada
[c] Department of Physics and Astronomy, University of British Columbia, 6224 Agricultural Road, Vancouver V6T 1Z1, Canada
[d] International Collaboration on Repair Discoveries (ICORD), University of British Columbia, 818 West 10th Avenue, Vancouver, BC V5Z 1M9, Canada
[e] Applied Statistics and Data Science Group (ASDa), Department of Statistics, University of British Columbia, 3178-2207 Main Mall, Vancouver, V6T 1Z4, Canada
[f] School of Biomedical Engineering, University of British Columbia, 251 - 2222 Heath Sciences Mall, Vancouver V6T 1Z3, Canada
[g] Department of Pathology & Laboratory Medicine, University of British Columbia, 2211 West Mall, Vancouver V6T 2B5, Canada
[h] Prothena Biosciences, 331 Oyster Point Boulevard, South San Francisco, CA 94080, USA
[i] F. Hoffmann-La Roche Ltd, Grenzacherstrasse 124, Basel 4070, Switzerland
[j] Genentech, Inc., 1 DNA Way, South San Francisco, CA 94080, USA

ARTICLE INFO

Keywords:
Myelin Water Imaging
Multiple Sclerosis
Ocrelizumab
Interferon Beta-1a
Demyelination
Remyelination

ABSTRACT

Background: Myelin water imaging is a magnetic resonance imaging (MRI) technique that quantifies myelin damage and repair in multiple sclerosis (MS) via the myelin water fraction (MWF).
Objective: In this substudy of a phase 3 therapeutic trial, OPERA II, MWF was assessed in relapsing MS participants assigned to interferon beta-1a (IFNb-1a) or ocrelizumab (OCR) during a two-year double-blind period (DBP) followed by a two-year open label extension (OLE) with ocrelizumab treatment.
Methods: MWF in normal appearing white matter (NAWM), including both whole brain NAWM and 5 white matter structures, and chronic lesions, was assessed in 29 OCR and 26 IFNb-1a treated participants at weeks 0, 24, 48 and 96 (DBP), and weeks 144 and 192 (OLE), and in white matter for 23 healthy control participants at weeks 0, 48 and 96.
Results: Linear mixed-effects models of data from baseline to week 96 showed a difference in the change in MWF over time favouring ocrelizumab in all NAWM regions. At week 192, lesion MWF was lower for participants originally randomised to IFNb-1a compared to those originally randomised to OCR. Controls showed no change in MWF over 96 weeks in any region.
Conclusion: Ocrelizumab appears to protect against demyelination in MS NAWM and chronic lesions and may allow for a more permissive micro environment for remyelination to occur in focal and diffusely damaged tissue.

1. Introduction

Conventional magnetic resonance imaging (MRI) outcomes used in multiple sclerosis (MS) clinical trials are sensitive for demonstrating suppression of new focal inflammation (new or enlarging T2 lesions and gadolinium enhancing T1 lesions). However, diffuse damage beyond lesions is typically only indirectly addressed by global measures such as progressive brain atrophy. Quantitative or advanced MRI techniques can

Abbreviations: MRI, magnetic resonance imaging; MS, multiple sclerosis; MWF, myelin water fraction; OCR, ocrelizumab; INF, interferon beta-1a; DBP, double-blind period; OLE, open label extension; NAWM, normal appearing white matter; MWI, myelin water imaging; 3DT1, three dimensional T1-weighted image; PDw, proton density weighted image; FLAIR, fluid attenuated inversion recovery; ROI, region of interest; CC, corpus callosum; CST, cortico-spinal tract; ILF, inferior longitudinal fasciculus; SLF, superior longitudinal fasciculus.

* Corresponding author at: S199 2211 Wesbrook Mall, University of British Columbia, V6T 2B5, Canada.
E-mail address: Shannon.Kolind@ubc.ca (S. Kolind).

[1] Equal contributions.

https://doi.org/10.1016/j.nicl.2022.103109
Received 22 April 2022; Received in revised form 27 June 2022; Accepted 10 July 2022
Available online 19 July 2022

investigate tissue-specific neuroprotective effects of MS therapies beyond prevention of new lesion formation and slowing of global atrophy. Studying myelin is of particular interest given this is the primary target of damage in MS and a focus for remyelinating and neuroprotective therapies.

Myelin water imaging (MWI) is a quantitative, myelin-specific MRI technique that separates the MRI signal into contributions from sub-voxel anatomical water pools (Deoni et al., 2008; MacKay et al., 1994). In central nervous system tissue, these water pools correspond to intra- and extra-cellular water, which relaxes slowly, and water trapped between the myelin bilayers, which relaxes more quickly (Mackay and Laule, 2016). The myelin-associated water signal fraction, termed the myelin water fraction (MWF) is used to investigate myelin damage and repair in MS, as well as other diseases in which myelin pathology is suspected (Mackay and Laule, 2016), and has been proposed as an outcome measure for clinical trials targeting remyelination and neuroprotection (Oh et al., 2019).

Ocrelizumab (OCR) is a B-cell-depleting monoclonal antibody that has shown greater efficacy at preventing clinical relapses, disability progression, and new focal inflammatory lesions on brain MRI relative to interferon beta-1a (IFNb-1a) in Phase III trials in relapsing MS (OPERA I and OPERA II) (Hauser et al., 2017). Further, earlier and continuous OCR treatment for up to 5 years provided sustained benefit on clinical and MRI measures of disease progression compared to participants who switched from IFNb-1a to OCR after a 2-year double-blind period (DBP) (Hauser et al., 2020). In this single-site substudy of OPERA II, we investigated whether myelin-related microstructural changes occur in OCR and IFNb-1a treated participants. MWI was used to evaluate myelin health and repair of chronic lesions and normal appearing white matter (NAWM) in participants randomized to OCR or IFNb-1a and followed for 4 years. Age and sex matched healthy controls were also followed for 2 years.

2. Methods

2.1. Participants

MS participants recruited into the OPERA II (clinical-trials.gov NCT01412333) double-blind, double-dummy, active control relapsing MS trial of OCR (600 mg IV every 24 weeks) versus IFNb-1a (44 mcg subcutaneous, three injections weekly) (Hauser et al., 2017) at the University of British Columbia (Vancouver, Canada) were invited to participate in an advanced MRI substudy. During the DBP, advanced MRI was performed at baseline (week 0), week 24, week 48 and week 96. During the open label extension (OLE) phase of the trial, where participants maintained or switched to OCR, advanced MRI was performed at week 144 and week 192. A cohort of age and sex matched healthy controls were recruited as a reference to standardize MS participant findings for physiological, non-MS-related changes in MWI measures. Healthy controls were recruited through referrals from site staff and subjects participating in the Phase III parent study. Poster advertisements and pamphlets located throughout the hospital were also used to assist with the recruitment of controls. For healthy controls, brain MRI was performed at baseline (week 0), and weeks 48, and 96. The UBC Clinical Research Ethics Board approved the trial and the substudy protocol (H11-02278) and all participants provided written informed consent.

2.2. MRI data acquisition

All participants were scanned with an 8-channel phased array head coil on a 3.0 T Philips Achieva MRI system (Best, The Netherlands). The MWI sequence used was the multi-component driven equilibrium single pulse observation of T1/T2 (mcDESPOT) (Deoni et al., 2013). This sequence allows rapid acquisition of high-resolution whole-brain data, which is then processed to yield quantitative maps from which MWF can be extracted. The mcDESPOT protocol was composed of a series of sagittally oriented spoiled gradient recalled echo (SPGR) and balanced steady-state free procession (bSSFP) acquisitions across a range of flip angles (α) as well as an inversion-recovery-prepared SPGR (IR-SPGR) scan for correction of flip angle inhomogeneity (Deoni, 2011). Scan parameters for the individual sequences were: SPGR: repetition time (TR) = 6.5 ms, echo time (TE) = 3.6 ms, flip angle (α) = [2, 3, 4, 6, 9, 13, 18]°; bSSFP: TR = 5.8 ms, TE = 2.9 ms, α = [7, 11, 15, 19, 24, 30, 47]°; IR-SPGR: TR = 6.5 ms, TE = 3.2 ms, α = 5°, inversion time (TI) = 450 ms, for the bSSFP volumes, all flip angles were acquired with phase-cycling patterns of 0° and 180° for correction of off-resonance effects (Deoni, 2011). A common isotropic voxel size of 1.7 × 1.7 × 1.7 mm^3 and field of view (FOV) of 220 × 160 × 220 mm^3 were used for SPGR, bSSFP and IR-SPGR scans. A 3D T_1-weighted scan ($3DT_1$) (TR = 28 ms, TE = 4 ms, α = 27°, voxel size = 1 × 1 × 3 mm^3, FOV = 250 × 188 × 180 mm^3, 60 slices) was collected for image registration and white matter segmentation.

For lesion identification, a proton density weighted (PDw) (TR = 2000 ms, TE = 10 ms, 60 slices, voxel size = 1 × 1 × 3 mm^3, FOV = 250 × 200 × 180 mm^3, echo train length [ETL] = 3), a T_2-weighted (T_2w) (TR = 6100 ms, TE = 80 ms, 60 slices, voxel size = 1 × 1 × 3 mm^2, FOV = 250 × 188 × 180 mm^3, ETL = 8), and a fluid attenuated inversion recovery (FLAIR) (TR = 9000 ms, TE = 80 ms, TI = 2,500 ms, 60 slices, voxel size = 1 × 1 × 3 mm^2, FOV = 250 × 188 × 180 mm^3, ETL = 12) sequence were collected.

2.3. MRI data image processing, registration and analysis

MWF maps were calculated using the processing methods outlined in Deoni and Kolind (Deoni and Kolind, 2015); briefly, the SPGR and IR-SPGR scans were used for DESPOT1 with High-speed Incorporation of RF Field Inhomogeneities (DESPOT1-HIFI) analysis (Deoni, 2007), resulting in maps of the global quantitative T1 and the B1 field. The bSSFP data and the global quantitative T1 and B1 maps were then used to calculate global T2 and B0 field maps using DESPOT2 with full modeling (DESPOT2-FM) analysis (Deoni, 2009). Finally, the B0 and B1 maps combined with the SPGR and bSSFP (with both phase-cycling schemes) were used to calculate the MWF using stochastic region contraction (Deoni and Kolind, 2015).

For each participant, a subject-specific template was created using the high flip-angle T1-weighted SPGR images from all the DBP time points, using ANTs (Advanced Normalization (Avants et al., 2011)). The MWF, 3DT1 and PDw images at each time point were then registered to this template using either ANTs (PDw, MWF) or FLIRT (FMRIB's Linear Image Registration Tool) (Zhang et al., 2001) from the FSL (Fmrib Software Library) toolbox (3DT1).

Lesions were identified on the T2w, PDw, and FLAIR for each subject at each time point by an experienced radiologist, placing one or more seed points where a lesion was identified. Segmentation was then performed automatically using the provided seed points according to the method described by Tam et al. (Tam et al., 2011) and McAusland et al. (McAusland et al., 2010) For the MS cohort, the subject's lesion masks were registered to the subject's template. Two lesion masks were then created. A chronic lesion mask was created by multiplying together all lesion masks to only retain lesion voxels common to all time points (intersection). A total lesion mask, which included all voxels labeled as lesion regardless of time point, was created by summing all the lesion masks (union).

White matter tissue masks were created using the segmentation tool FLIRT on the registered $3DT_1$ images. For MS participants, lesions were removed from the white matter tissue mask (resulting in a NAWM mask) by subtracting the total lesion mask at each time point. In addition, white matter anatomical regions of interest (ROIs), defined in standard space using the John Hopkins University (JHU) probabilistic tractography atlas (Hua et al., 2008), were registered to the subject-specific template. Four major white matter bundles were selected a priori

based on having a substantial number of pixels, reliable segmentation for brains with a potentially large amount of atrophy, and known involvement in MS: corpus callosum (CC), cortico-spinal tract (CST), inferior longitudinal fasciculus (ILF), and superior longitudinal fasciculus (SLF). These regions were multiplied by each participant's NAWM tissue mask to ensure only NAWM was included.

2.4. Statistical analysis

Student's t-tests were used to test for differences in age, disease duration and EDSS between groups. A $\chi 2$ test was used to determine whether the groups were matched for sex. Linear mixed effects models were used to account for repeated MWF measures over time on each subject and to handle incomplete longitudinal data. The linear mixed effects regression model was $Y_{ijk} = \mu + T_i + W_i + (TW)_{ij} + \eta_k + \varepsilon_{ijk}$ where y_{ijk} is the MWF for the i^{th} treatment (T_i), j^{th} week (W_j) and k^{th} subject. The visit week and treatment arms were kept as fixed effects while the subject was set as a random effect to account for individual variability. The random effects for subject (η_k) were independent and identically distributed across treatments. An interaction effect between week and treatment arm was included and type III ANOVA using the Satterthwaite approximation for the degrees of freedom used to test for an interaction effect. Additional fixed effects models were fit to percent change in MWF and one-way ANOVA and the Tukey method for multiple comparisons were used to assess group differences. All analyses were performed using R ("R: The R Project for Statistical Computing," n.d.). All tests were two-sided. As this analysis was exploratory, except for the mentioned adjustment in fixed effects models, no correction for multiple comparisons was made, and p-values are provided without a strict definition of significance (Statistical Association, 2016; Wasserstein and Lazar, 2016).

3. Results

3.1. Participant characteristics

Fifty-eight MS participants and 24 healthy controls were recruited into the MRI substudy. Four were excluded from study analysis: 2 MS participants with baseline scans only, 1 MS participant with only baseline and week 24 scans (randomized to OCR) and 1 healthy control with excessive motion artefacts. Data from some time points were missing due to lack of scan time, missed appointments or metal artefact due to new dental work (5 baseline, 1 week 24, 1 week 48, 5 week 144 and 5 week 192).

The baseline clinical and demographic characteristics of healthy controls and participants with MS are displayed in Table 1. MS participants and control groups were similar in age and sex distributions. The MS treatment groups were balanced at baseline in terms of disease duration, EDSS score and chronic lesion volume.

Table 1
Clinical and demographic characteristics.

	IFNb-1a (n = 28)	OCR (n = 27)	p	Controls (n = 23)	p*
Age in years, mean (range)	38 (18–56)	38 (22–56)	0.9	37 (19–56)	0.7
Females, n (%)	18 (64)	16 (59)	0.7	15 (65)	0.7
Disease Duration in years, mean (range)	4 (0–18)	3 (0–21)	0.6	NA	NA
EDSS, median (range)	2.0 (1.0–4.0)	2.0 (0.0–4.5)	0.6	NA	NA
Chronic lesion volume in mm^3, mean (standard deviation)	1408 (1348)	1860 (3209)	0.5	NA	NA

EDSS = Expanded Disability Status Scale, IFNb-1a = interferon β-1a, OCR = ocrelizumab, n = number of participants, p = p-value, NA = not applicable.
* *t*-test between Controls and all MS.

3.2. Changes in myelin water fraction during the double-blind period

3.2.1. Normal appearing white matter

No difference in MWF at baseline between IFNb-1a and OCR groups was found in any region. From the mixed-effects models fit to data from baseline to week 96, the treatment-by-visit interaction for MWF in all regions supported a difference in the change in MWF over time between treatment groups favouring ocrelizumab (CC p = 0.008, CST p = 0.03, ILF p = 0.02, SLF p = 0.02, all NAWM p = 0.05). Changes in MWF over time are shown in Fig. 1 for both treatment groups as well as healthy controls. While the MWF values were generally lower in MS NAWM than healthy control white matter, the point estimates from the mixed-effects models during the DBP suggest that MWF increased or remained stable in all regions for participants randomized to OCR and decreased in all regions for participants assigned to IFNb-1a.

One-way ANOVA revealed differences in the percent MWF change between IFNb-1a, OCR and healthy control groups in the CC (p = 0.009), CST (p = 0.02), ILF (p = 0.03) and SLF (p = 0.04), but not NAWM (p = 0.19). The mean MWF percentage changes from baseline to week 96 and p-values for Tukey contrasts are illustrated in Fig. 2 and listed in Table 2.

3.2.2. Chronic lesions

From week 0 to week 96, MWF increased (+1.0 %) in chronic lesions in the group assigned to OCR and decreased (-2.2 %) in those taking IFNb-1a (p = 0.11). The p-value for the treatment by time interaction during the DBP was 0.13. Change in MWF over time and group differences in chronic lesions are displayed in Fig. 3 and listed in Table 2.

3.3. Changes in myelin water fraction during the open label extension

3.3.1. Normal appearing white matter

Fig. 1 visually demonstrates that participants who switched from IFNb-1a to OCR, MWF appeared to stabilize or increased in all NAWM regions from week 96 to week 192, and MWF appeared to remain stable for participants who remained on OCR since baseline. Mean MWF percentage change from week 96 to week 192 are listed in Table 2 for all regions.

When considering the entire 4-year study period (DBP plus OLE), NAWM regions demonstrated treatment-by-time interaction with the following p-values: CC p = 0.05, CST p = 0.06, ILF p = 0.04, SLF p = 0.05, all NAWM p = 0.07 (Fig. 1) favouring continuous treatment with OCR from baseline to week 192. The point estimates for MWF in participants treated with OCR suggested a tendency to increase or remain stable in most ROIs, whereas participants who switched from IFNb-1a to OCR (IFNb-1a/OCR) for the OLE had larger overall decreases in MWF (Fig. 1 and Table 2). Fig. 2 illustrates the mean percent change in MWF in the treatment groups over the entire study period.

3.3.2. Chronic lesions

In participants who switched from IFNb-1a to OCR, MWF decreased (-2.8 %) in chronic lesions from week 96 to 192. Conversely, MWF remained unchanged (-0.4 %) in chronic lesions in the group assigned to OCR from baseline. A comparison of these MWF changes between treatment groups yielded p = 0.09, however, the treatment-by-time interaction had a p-value of 0.3. From week 0 to week 192, MWF increased (+1.5 %) in the group assigned to OCR at baseline and decreased (-3.7 %) in those who switched from IFNb-1a to OCR during the OLE (p = 0.02 comparing between the treatment groups); the treatment-by-time interaction had p = 0.08. Change in MWF over time and group differences in chronic lesions over the 4-year study period are displayed in Fig. 3 and listed in Table 2.

4. Discussion

Ocrelizumab has previously been demonstrated to have greater efficacy at preventing clinical relapses, disability progression, and new

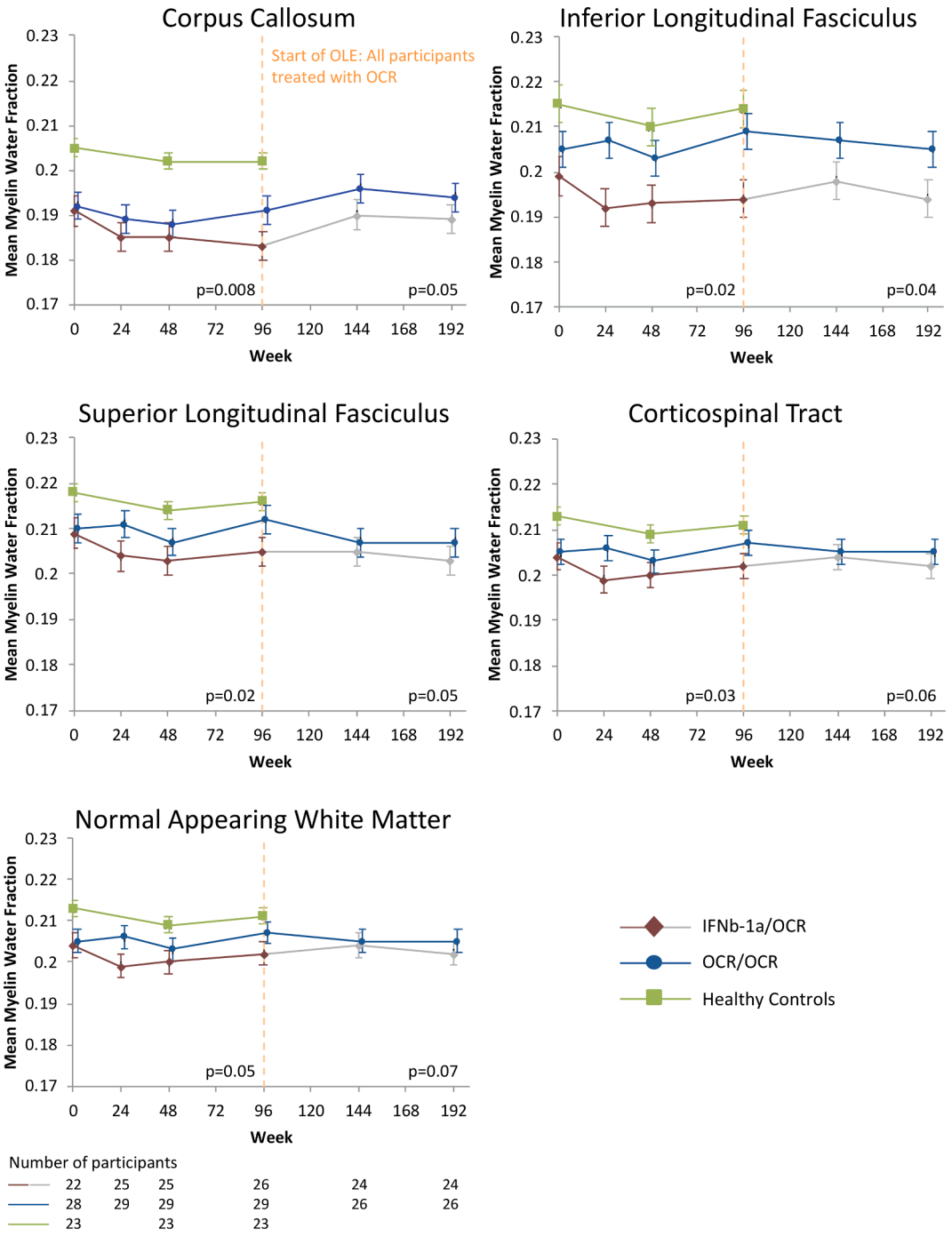

Fig. 1. Mixed model mean myelin water fraction (±Standard Error) over time in different white matter regions of interest for the participant groups: 1) Interferon beta 1a (IFNb-1a) from baseline to week 96 switching to ocrelizumab (OCR) from week 96 to week 192, 2) OCR from baseline to week 192 and 3) healthy controls from baseline to week 96. P-values indicate treatment-by-visit interactions for the double-blind period (weeks 0–96, left) and full 4 year study (weeks 0–192, right) from the mixed effects model. The number of participants at each time point is shown under the last plot. The vertical dashed line shows the time point at which IFNb-1a participants switched to OCR.

focal inflammatory lesions on brain MRI compared to interferon beta-1a during the 2-year DBP of the parent OPERA trial in relapsing MS (Hauser et al., 2017). Data from our present advanced MRI substudy suggest that ocrelizumab prevents demyelination in NAWM and in chronic lesions compared to interferon beta-1a. Some areas demonstrated increased MWF over time, further suggesting that ocrelizumab may create a more permissive environment for remyelination to occur in both focal and diffusely damaged tissue. Conversely, interferon beta-1a, while previously shown also to be an effective therapy at decreasing the risk of clinical relapses and new focal MRI lesions, demonstrated decreased MWF over time in chronic lesions and throughout the NAWM. This differential effect on myelin may, in part, account for the reduction in rate of brain atrophy and improved clinical outcomes seen in ocrelizumab versus interferon beta-1a treated participants reported in the broader OPERA I and II trial populations (Hauser et al., 2020; Hauser et al., 2017).

Additional data during the OLE phase further demonstrates continued stability of MWF in those treated from baseline with ocrelizumab. Participants switching from interferon beta-1a to ocrelizumab showed possible increases or stability in MWF in NAWM regions,

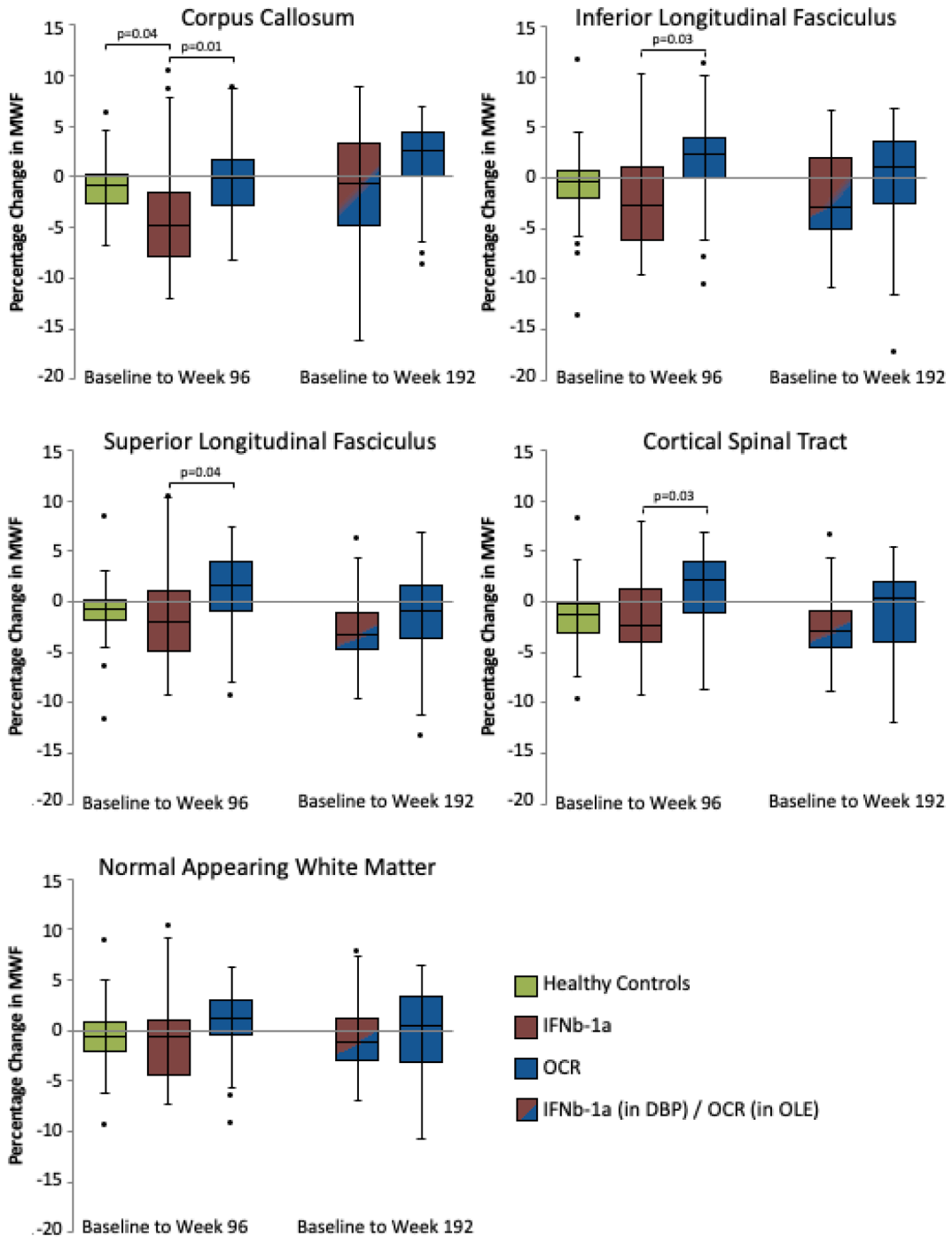

Fig. 2. Boxplots showing the percent change in MWF in different white matter regions of interest from baseline to week 96 and baseline to week 192 for healthy controls and two treatment arms: 1) interferon beta 1a (IFNb-1a) from baseline to week 96 switching to ocrelizumab (OCR) from week 96 to week 192 and 2) OCR from baseline to week 192. For clarity, only p-values < 0.05 between treatment using an ANOVA are indicated; all p-values are listed in Table 2.

although perhaps never reaching the same level as the ocrelizumab group at year 4, supporting the notion that earlier treatment with ocrelizumab may lead to better outcomes for people living with MS. In chronic lesions, MWF decreased by year 4 in those participants started on interferon beta-1a while it remained stable in the group assigned to ocrelizumab at baseline.

We hypothesize that one of the main mechanisms of action of ocrelizumab is anti-inflammatory and any neuroprotection would likely be secondary to that effect. An interesting result of this study is the impact on NAWM MWF, in part because the mechanisms of progressive NAWM demyelination are not fully elucidated. However, this data suggests that anti-inflammatory therapies might affect those mechanisms.

In the case of switching from interferon beta-1a to ocrelizumab, the difference in MWF at week 192 (end of study) look similar to the group on ocrelizumab throughout the study for NAWM (Fig. 1). However, when looking at individual ROIs (Figs. 1 and 2) the difference is more apparent. Normal MWF values are heterogenous from region to region throughout the brain (Dvorak et al., 2021b; O'Muircheartaigh et al., 2019), and group differences can be missed if larger composite regions are used to calculate outcome measures. Results from this study suggest that using separate white matter regions could increase the precision of estimates and the power of comparisons, improving the power to detect

Table 2
Fixed effects model estimates (95% confidence interval) for myelin water fraction percentage change from baseline to week 96, week 96 to week 192 and baseline to week 192 in each region of interest divided by treatment arm. Participants originally randomized to interferon beta 1a from baseline to week 96 were switched to open label ocrelizumab from week 96 to week 192.

ROI	Baseline to Week 96 Treatment			p	Week 96 to Week 192 Treatment		p	Baseline to Week 192 Treatment		p
	HC	IFNb-1a	OCR		IFNb-1a/OCR	OCR/OCR		IFNb-1a/OCR	OCR/OCR	
CC	−1.0 (-2.8, 0.7)	−4.0 (-5.8, −2.3)	−0.4 (-2.0, 1.1)	0.009	3.6 (1.8, 5.3)	1.8 (0.1, 3.6)	0.17	−1.2 (-3.5, 1.2)	1.5 (-0.6, 3.6)	0.09
ILF	−0.8 (-2.9, 1.4)	−2.1 (-4.5, 0.3)	1.9 (-0.3, 4.1)	0.03	0.4 (-1.6, 2.3)	−1.9 (-3.9, 0.03)	0.11	−2.1 (-4.5, 0.3)	0.03 (-2.1, 2.2)	0.18
SLF	−1.1 (-2.8, 0.6)	−1.8 (-3.7, 0.1)	1.2 (-0.5, 2.9)	0.04	−0.9 (-2.7, 0.8)	−2.5 (-4.2, −0.9)	0.19	−2.9 (-4.7, −1.0)	−1.5 (-3.2, 0.1)	0.29
CST	−1.4 (-3.0, 0.2)	−1.7 (-3.4, −0.07)	1.2 (-0.3, 2.6)	0.02	−0.7 (-2.5, 1.0)	−2.1 (-3.7, −0.4)	0.27	−2.5 (-4.2, −0.7)	−1.0 (-2.6, 0.6)	0.23
NAWM	−0.7 (-2.3, 0.9)	−1.1 (-2.8, 0.6)	0.8 (-0.7, 2.3)	0.19	0.6 (-1.0, 2.1)	−0.8 (-2.3, 0.7)	0.21	−0.7 (-2.5, 1.1)	−0.2 (-1.7, 1.4)	0.63
LES	–	−2.2 (-5.2, 0.7)	1.0 (-1.6, 3.6)	0.11	−2.8 (-5.8, 0.3)	−0.4 (-3.1, 2.3)	0.09	−3.7 (-7.0, −0.5)	1.5 (-1.4, 4.4)	0.02

ROI = region of interest, CC = corpus callosum, CST = cortical spinal tract, SLF = superior longitudinal fasciculus, ILF = inferior longitudinal fasciculus, NAWM = normal appearing white matter, LES = lesion, HC = healthy controls, IFNb-1a = interferon β-1a, OCR = ocrelizumab.

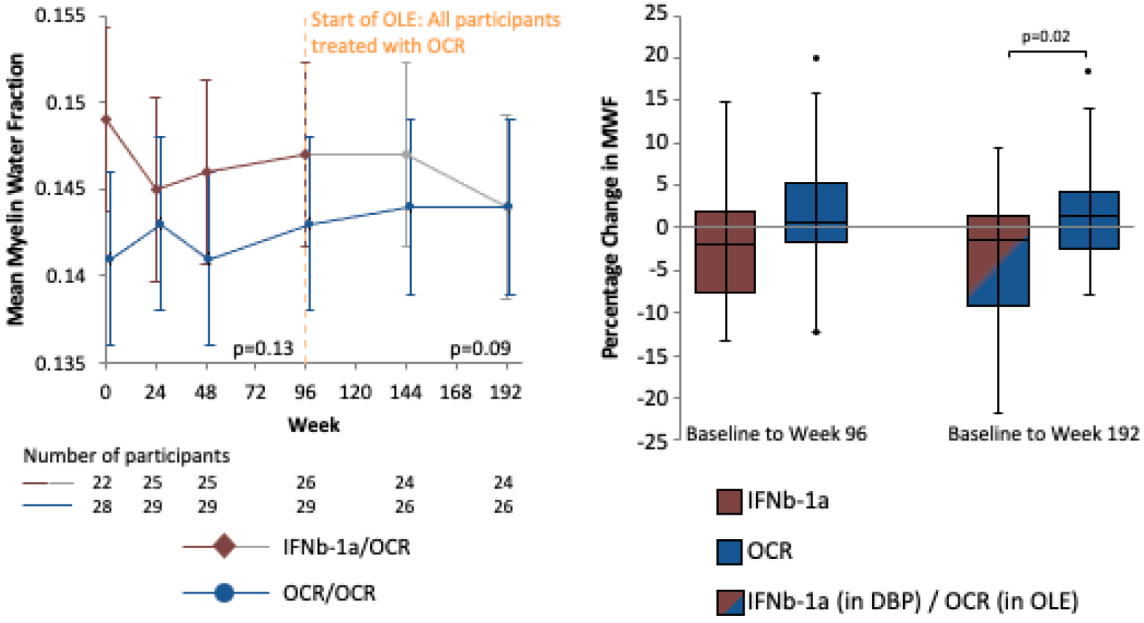

Fig. 3. Mixed model mean myelin water fraction (±Standard Error) over time (left plot) in chronic lesions for the two treatment arms: 1) interferon beta 1a (IFNb-1a) from baseline to week 96 switching to ocrelizumab (OCR) from week 96 to week 192 and 2) OCR from baseline to week 192. Boxplots (right plot) showing the percent change in MWF in chronic lesions from baseline to week 96 and baseline to week 192 for each treatment arm. The vertical dashed line shows the time point at which IFNb-1a participants switched to OCR. P-values in the left plot indicate treatment-by-visit interactions for the double-blind period (weeks 0–96, left) and full 4-year study (weeks 0–192, right) from the mixed effects model. The p-value in the right plot indicates a significant difference between treatment using an ANOVA. The number of participants at each time point is shown under the left plot.

treatment effects. We believe this data supports the brain atrophy data in the overall study population, where an atrophy benefit of ocrelizumab vs interferon beta-1a develops in the DBP and is maintained in the OLE. (Hauser et al., 2020; Hauser et al., 2017).

The MWF results are consistent with previous studies in relapsing MS, in demonstrating reduced MWF values in lesions and NAWM compared to healthy control white matter (Kolind et al., 2012; Laule et al., 2004; O'Muircheartaigh et al., 2019) and significant decreases over time without treatment or on first line therapies over as short of a period as 1 year (Matthews et al., 2015; Pandya et al., 2020; Vavasour et al., 2018). A study of 42 relapsing MS patients demonstrated no significant change in MWF values in lesions nor NAWM over 2 years upon initiating treatment with alemtuzumab (Vavasour et al., 2019), demonstrating greater stability than has been reported previously in groups on first line therapies or without treatment, although this study did not have a direct comparator group.

While MWF is generally considered to provide the most specific measure of myelin using MRI (Lazari and Lipp, 2021; Mancini et al., 2020; Oh et al., 2019), other studies of therapies applied to relapsing MS have included myelin-sensitive measures such as the magnetization transfer ratio (MTR), which decreases with demyelination and increases with remyelination, but is also sensitive to other effects such as inflammation and edema (Vavasour et al., 2011). In new lesions, a positive effect on MTR was shown for GSK239512 compared to placebo (Schwartzbach et al., 2017) and for glatiramer acetate relative to interferon beta-1a (Brown et al., 2016), while laquinimod showed a positive effect compared to placebo on MTR in normal appearing brain tissue, white matter, and grey matter, but not lesions (Filippi et al., 2014). Looking at voxelwise changes in MTR in normal appearing brain tissue, a larger number of voxels increasing in MTR (interpreted as

remyelination) and small number decreasing in MTR (interpreted as demyelination) were found for natalizumab compared to interferon beta-1a (Zivadinov et al., 2012). The results of our study are in line with these previous demonstrations but provide increased specificity and possibly sensitivity, detecting positive changes in a relatively small cohort in tissue with chronic damage.

The relatively small sample size was the main limitation of this study. However, even with small numbers in each treatment arm, differences in the percentage change in MWF over only 2 years were measured and participants treated with ocrelizumab had longitudinal MWF results that were more similar to healthy controls or even hinting at increases over time, although a larger sample or longer period is required to verify this promising suggestion. The mcDESPOT acquisition employed here used a limited range and number of flip angles; while this approach has been previously shown to produce results in line with the standard acquisition protocol (Dvorak et al., 2021a; O'Muircheartaigh et al., 2019), this may have led to less stability in fitting, weakening the consistency of results between voxels or individuals. The analysis approach used here was determined prior to beginning the clinical trial substudy; future work could implement more recent developments including TEC-mcDESPOT (Bouhrara and Spencer, 2015) and BMC-mcDESPOT (Bouhrara and Spencer, 2017), which could also increase the reliability of the measures. MWF values have been shown to be influenced by factors including APOE genotype and obesity; while these factors may have had a small impact on differences between participants with MS and controls, it is unlikely that this effect would be dominant or differ greatly between treatment groups. MWF changes can also be influenced by changes in water content, which may have contributed to the observed initial drop at week 24 in MWF for the interferon beta-1a group; however, it has been shown that the effects of total water content changes on MWF are minimal (Laule et al., 2004; Vavasour et al., 2021).

The advantages of a concurrent longitudinal healthy control group and the use of a single centre increase the confidence that the observed changes are not due to technical variables alone. Given that MWI is feasible for multicentre studies (Lee et al., 2018; Meyers et al., 2013), this study supports the role of using myelin water fraction as an outcome measure in clinical trials that focus on treatments that prevent demyelination or enhance remyelination in acute and chronic lesions and globally. Future work will explore the relationship between changes in MWF in NAWM and new lesion formation, as well as the effect of treatment on different types of lesions or areas of NAWM that may be more or less likely to remyelinate, for example examining "smouldering" (slowly expanding/phase-rim) lesions (Elliott et al., 2020), or distance/gradient of NAWM from lesions/ventricles. These studies will shed further light on the biological underpinnings inherent to the tissue as well as mechanism of action for treatment. A voxel-wise, z-score approach may also be employed to further explore spatial relationships with myelin changes in relation to progression.

Funding

This work was funded by F. Hoffmann-La Roche ltd. SK was supported by Michael Smith Health Research BC.

CRediT authorship contribution statement

Shannon Kolind: Conceptualization, Data curation, Formal analysis, Funding acquisition, Investigation, Methodology, Project administration, Resources, Software, Supervision, Writing – original draft, Writing – review & editing. **Shawna Abel:** Formal analysis, Visualization, Writing – original draft. **Carolyn Taylor:** Formal analysis, Investigation, Methodology, Writing – review & editing. **Roger Tam:** Conceptualization, Methodology, Resources, Supervision, Writing – review & editing. **Cornelia Laule:** Conceptualization, Methodology, Writing – review & editing. **David K.B. Li:** Conceptualization, Methodology, Writing – review & editing. **Hideki Garren:** Conceptualization, Methodology, Writing – review & editing. **Laura Gaetano:** Writing – review & editing. **Corrado Bernasconi:** Formal analysis, Methodology, Writing – review & editing. **David Clayton:** Conceptualization, Methodology, Resources, Writing – review & editing. **Irene Vavasour:** Conceptualization, Data curation, Formal analysis, Investigation, Methodology, Project administration, Resources, Software, Supervision, Visualization, Writing – original draft, Writing – review & editing. **Anthony Traboulsee:** Conceptualization, Data curation, Funding acquisition, Investigation, Methodology, Project administration, Resources, Supervision, Visualization, Writing – original draft, Writing – review & editing.

Declaration of Competing Interest

S Kolind has received research support from Biogen, Roche and Sanofi Genzyme and consulting fees from Novartis and Roche. D Li has been a consultant to Vertex Pharmaceuticals and Genzyme, served on the Scientific Advisory Board for Celgene and the PML-MS Steering Committee for Biogen, and given lectures, supported by non-restricted education grants from Academy of Health Care Learning, Consortium of MS Centers and Sanofi-Genzyme. H Garren is an employee of Prothena Biosciences, and was an employee of Genentech, Inc over the course of the study. L Gaetano is an employee of F. Hofmann-La Roche Ltd. C Bernasconi is a contractor of F. Hofmann-La Roche Ltd. D Clayton is an employee of Genentech, Inc. A Traboulsee has received research support from Sanofi Genzyme and Roche; has received consulting fees from Sanofi Genzyme, Roche, Teva Neuroscience, Novartis, Biogen and EMD Serono; and has received honoraria for his involvement in speaker bureau activities for Sanofi Genzyme and Roche.

Acknowledgements

The authors wish to thank the study participants, the UBC MRI Research Centre MR technologists, Dr. Nicholas Seneca for contributions to initiating the study, Dr. Rick White for statistical consultation, and the UBC MSMRI Research Group for lesion segmentation and data management.

References

R: The R Project for Statistical Computing [WWW Document], n.d. URL https://www.r-project.org/ (accessed 4.10.22).

Avants, B.B., Tustison, N.J., Song, G., Cook, P.A., Klein, A., Gee, J.C., 2011. A reproducible evaluation of ANTs similarity metric performance in brain image registration. Neuroimage 54, 2033–2044. https://doi.org/10.1016/J.NEUROIMAGE.2010.09.025.

Bouhrara, M., Spencer, R.G., 2015. Incorporation of nonzero echo times in the SPGR and bSSFP signal models used in mcDESPOT. Magn. Reson. Med. 74, 1227–1235. https://doi.org/10.1002/MRM.25984.

Bouhrara, M., Spencer, R.G., 2017. Rapid simultaneous high-resolution mapping of myelin water fraction and relaxation times in human brain using BMC-mcDESPOT. Neuroimage 147, 800–811. https://doi.org/10.1016/j.neuroimage.2016.09.064.

Brown, R.A., Narayanan, S., Stikov, N., Cook, S., Cadavid, D., Wolansky, L., Arnold, D.L., 2016. MTR recovery in brain lesions in the BECOME study of glatiramer acetate vs interferon β-1b. Neurology 87, 905–911. https://doi.org/10.1212/WNL.0000000000003043.

Deoni, S.C.L., 2007. High-Resolution T1 Mapping of the Brain at 3T with Driven Equilibrium Single Pulse Observation of T1 with High-Speed Incorporation of RF Field Inhomogeneities (DESPOT1-HIFI). J. Magn. Reson. Imaging 26, 1106–1111. https://doi.org/10.1002/jmri.21130.

Deoni, S.C.L., 2009. Transverse Relaxation Time (T 2) Mapping in the Brain With Off-Resonance Correction Using Phase-Cycled Steady-State Free Precession Imaging. J. Magn. Reson. Imaging 30, 411–417. https://doi.org/10.1002/jmri.21849.

Deoni, S.C.L., 2011. Correction of main and transmit magnetic field (B0 and B 1) inhomogeneity effects in multicomponent-driven equilibrium single-pulse observation of T1 and T2. Magn. Reson. Med. 65, 1021–1035. https://doi.org/10.1002/MRM.22685.

Deoni, S.C.L., Kolind, S.H., 2015. Investigating the stability of mcDESPOT myelin water fraction values derived using a stochastic region contraction approach. Magn. Reson. Med. 73, 161–169. https://doi.org/10.1002/mrm.25108.

Deoni, S.C.L., Rutt, B.K., Arun, T., Pierpaoli, C., Jones, D.K., 2008. Gleaning multicomponent T1 and T2 information from steady-state imaging data. Magn Reson Med 60, 1372–1387.

Deoni, S.C.L., Matthews, L., Kolind, S.H., 2013. One component? Two components? Three? The effect of including a nonexchanging "free" water component in multicomponent driven equilibrium single pulse observation of T1 and T2. Magn Reson Med 70, 147–154.

Dvorak, A. v., Ljungberg, E., Vavasour, I.M., Lee, L.E., Abel, S., Li, D.K.B., Traboulsee, A., MacKay, A.L., Kolind, S.H., 2021a. Comparison of multi echo T2 relaxation and steady state approaches for myelin imaging in the central nervous system. Scientific Reports 11. https://doi.org/10.1038/s41598-020-80585-7.

Dvorak, A. v., Swift-LaPointe, T., Vavasour, I.M., Lee, L.E., Abel, S., Russell-Schulz, B., Graf, C., Wurl, A., Liu, H., Laule, C., Li, D.K.B., Traboulsee, A., Tam, R., Boyd, L.A., MacKay, A.L., Kolind, S.H., 2021b. An atlas for human brain myelin content throughout the adult life span. Sci Rep 11. https://doi.org/10.1038/S41598-020-79540-3.

Elliott, C., Arnold, D.L., Chen, H., Ke, C., Zhu, L., Chang, I., Cahir-McFarland, E., Fisher, E., Zhu, B., Gheuens, S., Scaramozza, M., Beynon, V., Franchimont, N., Bradley, D.P., Belachew, S., 2020. Patterning Chronic Active Demyelination in Slowly Expanding/Evolving White Matter MS Lesions. AJNR Am. J. Neuroradiol. 41, 1–8. https://doi.org/10.3174/AJNR.A6742.

Filippi, M., Rocca, M.A., Pagani, E., de Stefano, N., Jeffery, D., Kappos, L., Montalban, X., Boyko, A.N., Comi, G., 2014. Placebo-controlled trial of oral laquinimod in multiple sclerosis: MRI evidence of an effect on brain tissue damage. J. Neurol. Neurosurg. Psychiatry 85, 852–859. https://doi.org/10.1136/JNNP-2013-306132.

Hauser, S.L., Bar-Or, A., Comi, G., Giovannoni, G., Hartung, H.-P., Hemmer, B., Lublin, F., Montalban, X., Rammohan, K.W., Selmaj, K., Traboulsee, A., Wolinsky, J. S., Arnold, D.L., Klingelschmitt, G., Masterman, D., Fontoura, P., Belachew, S., Chin, P., Mairon, N., Garren, H., Kappos, L., 2017. Ocrelizumab versus Interferon Beta-1a in Relapsing Multiple Sclerosis. N. Engl. J. Med. 376, 221–234. https://doi.org/10.1056/NEJMOA1601277.

Hauser, S.L., Kappos, L., Arnold, D.L., Bar-Or, A., Brochet, B., Naismith, R.T., Traboulsee, A., Wolinsky, J.S., Belachew, S., Koendgen, H., Levesque, V., Manfrini, M., Model, F., Hubeaux, S., Mehta, L., Montalban, X., 2020. Five years of ocrelizumab in relapsing multiple sclerosis: OPERA studies open-label extension. Neurology 95, e1854–e1867. https://doi.org/10.1212/WNL.0000000000010376.

Hua, K., Zhang, J., Wakana, S., Jiang, H., Li, X., Reich, D.S., Calabresi, P.A., Pekar, J.J., van Zijl, P.C.M., Mori, S., 2008. Tract probability maps in stereotaxic spaces: analyses of white matter anatomy and tract-specific quantification. Neuroimage 39, 336–347. https://doi.org/10.1016/J.NEUROIMAGE.2007.07.053.

Kolind, S., Matthews, L., Johansen-Berg, H., Leite, M.I., Williams, S.C.R., Deoni, S., Palace, J., 2012. Myelin water imaging reflects clinical variability in multiple sclerosis. Neuroimage 60, 263–270. https://doi.org/10.1016/J.NEUROIMAGE.2011.11.070.

Laule, C., Vavasour, I.M., Moore, G.R.W., Oger, J., Li, D.K.B., Paty, D.W., MacKay, A.L., 2004. Water content and myelin water fraction in multiple sclerosis. A T2 relaxation study. J. Neurol. 251, 284–293. https://doi.org/10.1007/S00415-004-0306-6.

Lazari, A., Lipp, I., 2021. Can MRI measure myelin? Systematic review, qualitative assessment, and meta-analysis of studies validating microstructural imaging with myelin histology. Neuroimage 230. https://doi.org/10.1016/J.NEUROIMAGE.2021.117744.

Lee, L.E., Ljungberg, E., Shin, D., Figley, C.R., Vavasour, I.M., Rauscher, A., Cohen-Adad, J., Li, D.K.B., Traboulsee, A.L., Mackay, A.L., Lee, J., Kolind, S.H., 2018. Inter-Vendor Reproducibility of Myelin Water Imaging Using a 3D Gradient and Spin Echo Sequence. Front Neurosci. 12, 854.

Mackay, A.L., Laule, C., 2016. Magnetic Resonance of Myelin Water: An in vivo Marker for Myelin. Brain Plast 2, 71–91.

MacKay, A., Whittall, K., Adler, J., Li, D., Paty, D., Graeb, D., 1994. In vivo visualization of myelin water in brain by magnetic resonance. Magn Reson Med 31, 673–677.

Mancini, M., Karakuzu, A., Cohen-Adad, J., Cercignani, M., Nichols, T.E., Stikov, N., 2020. An interactive meta-analysis of MRI biomarkers of myelin. Elife 9, 1–23. https://doi.org/10.7554/ELIFE.61523.

Matthews, L., Kolind, S., Brazier, A., Leite, M.I., Brooks, J., Traboulsee, A., Jenkinson, M., Johansen-Berg, H., Palace, J., 2015. Imaging Surrogates of Disease Activity in Neuromyelitis Optica Allow Distinction from Multiple Sclerosis. PLoS ONE 10. https://doi.org/10.1371/JOURNAL.PONE.0137715.

McAusland, J., Tam, R.C., Wong, E., Riddehough, A., Li, D.K.B., 2010. Optimizing the use of radiologist seed points for improved multiple sclerosis lesion segmentation. IEEE Trans Biomed Eng 57, 2689–2698. https://doi.org/10.1109/TBME.2010.2055865.

Meyers, S.M., Vavasour, I.M., Mädler, B., Harris, T., Fu, E., Li, D.K.B., Traboulsee, A.L., Mackay, A.L., Laule, C., 2013. Multicenter measurements of myelin water fraction and geometric mean T2: intra- and intersite reproducibility. J. Magn. Reson. Imaging 38, 1445–1453. https://doi.org/10.1002/JMRI.24106.

O'Muircheartaigh, J., Vavasour, I., Ljungberg, E., Li, D.K.B., Rauscher, A., Levesque, V., Garren, H., Clayton, D., Tam, R., Traboulsee, A., Kolind, S., 2019. Quantitative neuroimaging measures of myelin in the healthy brain and in multiple sclerosis. Hum Brain Mapp 40, 2104–2116. https://doi.org/10.1002/HBM.24510.

Oh, J., Ontaneda, D., Azevedo, C., Klawiter, E.C., Absinta, M., Arnold, D.L., Bakshi, R., Calabresi, P.A., Crainiceanu, C., Dewey, B., Freeman, L., Gauthier, S., Henry, R., Inglese, M., Kolind, S., Li, D.K.B., Mainero, C., Menon, R.S., Nair, G., Narayanan, S., Nelson, F., Pelletier, D., Rauscher, A., Rooney, W., Sati, P., Schwartz, D., Shinohara, R.T., Tagge, I., Traboulsee, A., Wang, Y., Yoo, Y., Yousry, T., Zhang, Y., Sicotte, N.L., Reich, D.S., 2019. Imaging outcome measures of neuroprotection and repair in MS: A consensus statement from NAIMS. Neurology 92, 519–533. https://doi.org/10.1212/WNL.0000000000007099.

Pandya, S., Kaunzner, U.W., Hurtado Rúa, S.M., Nealon, N., Perumal, J., Vartanian, T., Nguyen, T.D., Gauthier, S.A., 2020. Impact of Lesion Location on Longitudinal Myelin Water Fraction Change in Chronic Multiple Sclerosis Lesions. J Neuroimaging 30, 537–543. https://doi.org/10.1111/JON.12716.

Schwartzbach, C.J., Grove, R.A., Brown, R., Tompson, D., Then Bergh, F., Arnold, D.L., 2017. Lesion remyelinating activity of GSK239512 versus placebo in patients with relapsing-remitting multiple sclerosis: a randomised, single-blind, phase II study. J Neurol 264, 304–315. https://doi.org/10.1007/S00415-016-8341-7.

Statistical Association, A., 2016. AMERICAN STATISTICAL ASSOCIATION RELEASES STATEMENT ON STATISTICAL SIGNIFICANCE AND P-VALUES. https://doi.org/10.1080/00031305.2016.1154108#.Vt2XIOaE2MN.

Tam, R.C., Traboulsee, A., Riddehough, A., Sheikhzadeh, F., Li, D., 2011. The impact of intensity variations in T1-hypointense lesions on clinical correlations in multiple sclerosis. Mult. Scler 17, 949–957. https://doi.org/10.1177/1352458511402113.

Vavasour, I.M., Laule, C., Li, D.K.B., Traboulsee, A.L., Mackay, A.L., 2011. Is the magnetization transfer ratio a marker for myelin in multiple sclerosis? J. Magn. Reson. Imaging 33, 713–718.

Vavasour, I.M., Huijskens, S.C., Li, D.K.B., Traboulsee, A.L., Mädler, B., Kolind, S.H., Rauscher, A., Moore, G.W., MacKay, A.L., Laule, C., 2018. Global loss of myelin water over 5 years in multiple sclerosis normal-appearing white matter. Mult. Scler. 24, 1557–1568. https://doi.org/10.1177/1352458517723717.

Vavasour, I.M., Tam, R., Li, D.K.B., Laule, C., Taylor, C., Kolind, S.H., MacKay, A.L., Javed, A., Traboulsee, A., 2019. A 24-month advanced magnetic resonance imaging study of multiple sclerosis patients treated with alemtuzumab. Mult Scler 25, 811–818. https://doi.org/10.1177/1352458518770085.

Vavasour, I.M., Chang, K.L., Combes, A.J.E., Meyers, S.M., Kolind, S.H., Rauscher, A., Li, D.K.B., Traboulsee, A., MacKay, A.L., Laule, C., 2021. Water content changes in new multiple sclerosis lesions have a minimal effect on the determination of myelin water fraction values. J Neuroimaging 31, 1119–1125. https://doi.org/10.1111/JON.12908.

Wasserstein, R.L., Lazar, N.A., 2016. The ASA's Statement on p-Values: Context, Process, and Purpose. Am. Stat. 70, 129–133. https://doi.org/10.1080/00031305.2016.1154108/SUPPL_FILE/UTAS_A_1154108_SM8096.PDF.

Zhang, Y., Brady, M., Smith, S., 2001. Segmentation of brain MR images through a hidden Markov random field model and the expectation-maximization algorithm. IEEE Trans. Med. Imaging 20, 45–57. https://doi.org/10.1109/42.906424.

Zivadinov, R., Dwyer, M.G., Hussein, S., Carl, E., Kennedy, C., Andrews, M., Hojnacki, D., Heininen-Brown, M., Willis, L., Cherneva, M., Bergsland, N., Weinstock-Guttman, B., 2012. Voxel-wise magnetization transfer imaging study of effects of natalizumab and IFNβ-1a in multiple sclerosis. Mult. Scler. 18, 1125–1134. https://doi.org/10.1177/1352458511433304.